SEMARAK ILMU PUBLISHING

Journal of Advanced Research in Applied Sciences and Engineering Technology

Journal homepage:
https://semarakilmu.com.my/journals/index.php/applied_sciences_eng_tech/index
ISSN: 2462-1943

Impact of Variation in Switching Frequency and Modulation Index on Z-Source Inverter Input Current

Kapil P. N.[1,2], Amit V. Sant[1,*]

[1] Department of Electrical Engineering, School of Technology, Pandit Deendayal Energy University, Gandhinagar, Gujarat, India
[2] Department of Electrical Engineering, School of Engineering, Nirma University, Ahmedabad, Gujarat, India

ABSTRACT

Many inverter topologies are used for industrial automation, electric vehicle charging stations, and grid integration for renewable energy. Of the different inverter configurations, the Z-Source Inverter (ZSI) receives attention in grid integration of battery and photovoltaic panels. This is due to the unique feature of ZSI, which allows for voltage boost operation in addition to the traditional *dc-ac* conversion. The power structure of ZSI includes an impedance network interfaced between the input *dc* source and the 3-leg inverter. Switching frequency and input *dc*-link voltage have an impact on the performance of the impedance network to start off with, which directly impacts the output characteristics of the inverter as well as the sizing of the components. The impact of the chosen switching frequency on the amount of *dc*-link current and voltage stress on power electronic switches and load is carefully analyzed in this work. The ideal best-fit values for various parameters, such as switching frequency, modulation index, shoot-through time, and amplitude of *dc*-link current on the power delivery of ZSI are also supplied with the pertinent mathematical formulas and MATLAB/SIMULINK-based validation. The paper aims to discuss the issues pertaining to the impact of the impedance network values on the energy supplied to and delivered by ZSI in terms of the current drawn at the input as well as the voltage obtained at the output. Through the presented work, an exact idea about the input current required by the ZSI can be determined, which can assist in the selection of the input source and its subsequent grid integration.

Keywords:
Modulation index; power converters; switching frequency; Z-source inverters

1. Introduction

The advent of high-power electronic devices has made it possible to convert and control electrical power in a variety of applications, including rectifiers, inverters, industrial drives, and HVDC transmission [1-4]. Through the implementation of a suitable inverter topology and control strategy, it is possible to convert the direct current (DC) power derived from energy storage devices like batteries, fuel cells, etc., as well as renewable energy sources such as solar and wind energy into controllable alternating current (AC) output. This *ac* output can then be seamlessly integrated into the existing electrical grid [5-6]. The impedance offered at the input of a voltage source

* *Corresponding author.*
E-mail address: amit.sant@sot.pdpu.ac.in

https://doi.org/10.37934/araset.57.2.7079

inverter (VSI) is small, but the output voltage is independent of the nature of the load. On the contrary, in the current source inverter (CSI), there is a huge input impedance connected between *dc* source and inverter power structure, enabling the input dc current to remain constant [5-6].

The voltage source-driven converter exhibits buck and boost operation when employed in inverter and rectifier modes, respectively. The CSI, in the context of this study, operates as a boost converter when functioning in the inverter mode, as described by [1-5]. There are certain limitations associated with VSI which include reduced *ac* voltage compared to input *dc* link as well as restriction in turning on complementary switches together in any leg as it may cause an imminent dead short circuit. A delay / dead band circuit between the gate pulses for the complimentary switches avoids the short circuit issue. The fall in output voltage occurs as a result of decreased use of the *dc* link in this operation. One limitation of CSI is that it is imperative to ensure that at least one switch from both the upper and lower sets remain closed, as leaving any of them open can result in detrimental effects on the source inductor and adversely affect electromagnetic interference (EMI) performance.

The ZSI possesses a unique characteristic that distinguishes it from other inverter topologies. Specifically, it has the capability to deliver an output voltage that can be either decreased or increased relative to the input *dc* link voltage. The characteristic feature of ZSI is achieved through the incorporation of a symmetrical impedance network comprising a switching inductor and capacitor. The input impedance network in the Z-source inverter serves the purpose of constraining the extent of *dc* link variation, achieving a level of voltage limitation that is comparable to that observed in the VSI. Users have the ability to activate a short-circuit state in the complementary pair of switches while simultaneously benefiting from the current limiting capability inherent in the CSI design Peng *et al.,* [1] and Rajakaruna *et al.,* [7].

Consequently, the resultant voltage is amplified, thereby augmenting the operating potential of the inverter. Furthermore, it provides a viable power conversion topology capable of modifying the output alternating current (*ac*) voltage to a specific level based on the direct current (*dc*) link input voltage. The determination of the output voltage level is contingent upon the short circuit states and their corresponding short circuit timings, as stated by Rajakaruna *et al.,* [7]. ZSI is employed due to its unique characteristics that enable it to overcome the limitations of conventional voltage source and current source inverters. The absence of an intermediate power converter step in the ZSI enables the adjustment of *ac* voltage, hence facilitating efficient operation.

The design of an impedance network consisting of a switching inductor and capacitor at the input of the inverter is an intricate process. Design for the said components depends on the amount of time for which the short circuit state is going to be continued within the ZSI during every switching cycle at the same time, and also depends on the amount of boost-up voltage to be obtained at the output of the ZSI based on the input *dc* voltage [8-10]. The selection of design parameters, apart from deciding the performance of ZSI, also provides a handful of relevant information in terms of the sizing and energy storage capability of the impedance network. The amount of energy stored and delivered by the impedance network as a whole, with individual contributions of switching inductor and capacitor, decides the domain of application for the inverter with its operational characteristics, which sheds light on the suitability of the components in regards to accommodating it in a practical system.

In this paper, a detailed analysis of the impact of switching frequency and modulation index on the input current drawn on *dc* side of ZSI is carried out. The analysis is done using the simulation tool as well as the mathematical design of the converter. The dependence of input *dc* current on various parameters is deduced, and accordingly, a detailed simulation study is conducted. The extent of impact of individual parameters on the input *dc* current is looked into and accordingly

summarized or tabulated such that inferences based on it can be drawn. The aim of the analysis carried out is to be able to visualize the change in output of the converter due to the parameter variation and also be able to correlate the impact of parameters on the sizing of the various magnetic components used in the formation of the impedance network. Results and findings are discussed with the help of graphs and waveforms for apt visualization. The best-fit values for the switching frequency, inductance, capacitance, and switching frequency can be obtained using the analysis presented in the paper. The purpose of this study is to explore the effects of the inductance and capacitance of the impedance network on the energy supplied to and delivered by ZSI in terms of the current drawn at the input and the voltage obtained at the output. Through the provided work, it is possible to get a precise understanding of the input current needed by the ZSI, which can help with the choice of the input source and subsequent grid integration.

2. ZSI: Power Topology, Control and Design

2.1 ZSI Power Topology

The construction of ZSI is comparable to a conventional three-phase bridge inverter with the exception of the presence of an impedance network consisting of an inductor and capacitor at *dc* link side. The power topology of the ZSI is shown in Figure 1. In comparison to the conventional inverter power structure, the ZSI contains nine distinct switch transitions that include six active output states, two zero output states, and one short circuit state (also called a shoot-through state) at the *dc* link side for output voltage enhancement [1-3]. The desired short circuit state of ZSI is produced by providing a gating pulse to both switches on one leg (complementary pair), and this modality can be carried out for one leg, two legs, or all three legs of the inverter. This shorts the supply terminals and creates the additional state leading to the extraction of higher output voltage. The said short circuit is not permitted in the VSI as it will short-circuit the *dc* link terminals leading to its damage on account of the low value of impedance provided by *dc* link side [11-13]. A total of seven possible short circuit states can be realized by either engaging the short circuit in one leg, two legs, or all three legs of the inverter. The realization of the short circuit states is ensured by the high input impedance provided by a symmetrical network made up of inductors and capacitors. For a particular *dc* link input, these short circuit states result in energy storage in the impedance network on the *dc* link side, which increases or decreases the inverter's output voltage [1-3, 7-8].

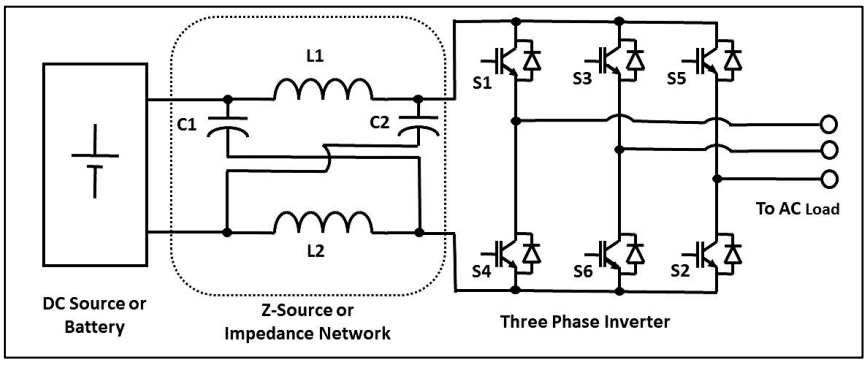

Fig. 1. Power topology of conventional Z-Source Inverter (ZSI)

2.2 Control Strategy

Traditionally, ZSI (Zero Sequence Injection) is regulated through the use of different control schemes, namely Simple Boost Control, Maximum Boost Control, and Maximum Constant Boost

Control. The control approach utilized to assess the relationship between input direct current and switching frequency and modulation index is known as Simple Boost Control (SBC) [9, 14-17]. In order to attain the required output voltage in a Switched Boost Converter (SBC), the active states are integrated with two adjacent active output states, zero output states, or short circuit states within each switching cycle, as determined by the switching frequency. The switches in each phase or legs operate during a switching cycle to achieve an even distribution of short circuit states while maintaining a consistent overall switching length [8, 9, 18-20]. The short circuit states can lead to the achievement of increased *ac* voltage compared to input *dc* voltage [21-25]. Figure 2 illustrates the process of PWM generation using a simple boost control technique.

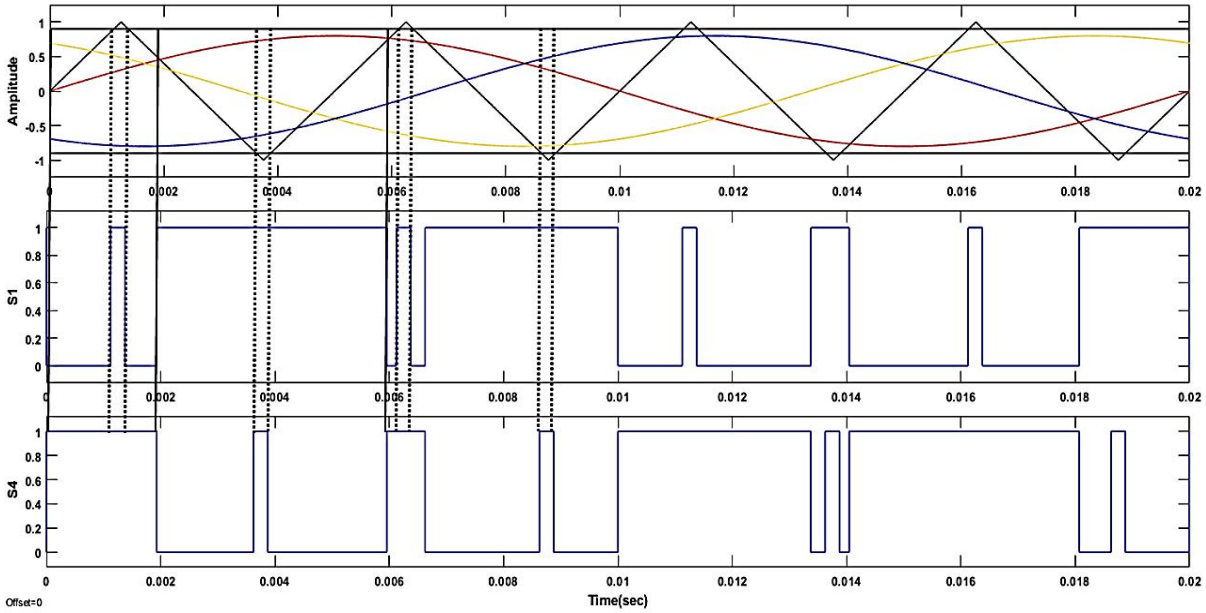

Fig. 2. Simple Boost Control (SBC) PWM scheme

2.3 Impedance Design of ZSI

On account of the short circuit state, ZSI incorporates the capability of buck-boost *dc-dc* converter along with that of the VSI. Selection of the inductors, L1 and L2, and capacitors, C1 and C2, of the impedance network is critical for the desired operation of the ZSI. Looking at the power structure of ZSI, it can be deduced that L1=L2=L and C1=C2=C as the circuit with impedance network is a symmetrical network [9, 10]. The design equations for the ZSI are derived by analyzing the active output, short circuit and zero output states [7-9]. The design equations having the contribution of V_i (inverter output voltage), M (modulation index), B (boosting factor), V_s (*dc* supply voltage), D_s (shoot-through duty ratio), T_o (shoot-through time), T_s (switching time) is derived based on the said concept and the same is mentioned below:

$$V_i = \frac{(M*B*V_s)}{2} \tag{1}$$

$$\frac{T_o}{T_s} = \frac{(2\pi - 3\sqrt{3}M)}{2\pi} \tag{2}$$

$$D_s = \frac{T_o}{T_s} \tag{3}$$

$$B = \frac{1}{(1-\frac{2T_o}{T_s})} \quad (4)$$

Also,

$$G = B.M \quad (5)$$

and

$$G = B.M = \frac{M}{1-2D_0} \quad (6)$$

By using equation 5 in equation 6,

$$B = \left(\frac{\pi}{3\sqrt{3}M-\pi}\right) \quad (7)$$

The Voltage gain, G, which is computed over one switching instant can be correlated with modulation index M as:

$$G = M * B = \left(\frac{\pi M}{3\sqrt{3}M-\pi}\right) \quad (8)$$

On combining the equations or relations, the expressions representing the values of impedance network components viz. inductance and capacitance can be expressed as:

$$C(in\mu F) = \frac{3*D_s*T_s*M*I_m*pf}{8*k_v*V_s*(1-D_s)*1000000} \quad (9)$$

$$L(inmH) = \frac{2*V_s*D_s*T_s*(1-D_s)}{3*K_i*M*I_m*pf} \quad (10)$$

where I_m (output current) is $\frac{P*1000}{V_s*pf}$, P is Power rating (range 1kW - 100kW), k_v is voltage ripple across capacitor (range 0.5 % - 10 %) and k_i = current ripple in the inductor (range 0.5 % - 10 %), pf is load power factor

3. Results

Based on the mathematical relations derived, it is indicative that B, M and f_{sw} are not decoupled and inter-related to each other. Figures 3, 4 and 5 shows the value of output voltage of ZSI and input *dc*-link current drawn for f_{sw} and M of 6 kHz & 0.9, 10 kHz & 0.9 and 20 kHz & 0.85 respectively. The selection of the modulation index and switching frequency is done based on the practical constraints normally followed in a power converter circuit. While fulfilling the requirement of output by the inverter at the application end, the order of voltage and current stress experienced by the switches and impedance component is something that cannot be ignored. The stress in-terms of current, voltage and heating play a vital role in effective or optimal performance of the circuit on the desired lines. This is the primary reason for selecting the above-mentioned values and accordingly the analysis is carried out on the simulation software or tool. Table 1 consolidates the results for *dc*-link voltage, V_{dc}, input *dc* current, I_{dc}, output voltage of ZSI, Vin, at M of 0.9. Table 2

consolidates the results for for dc-link voltage, V_{dc}, input dc current, I_{dc}, output voltage of ZSI, Vin, at different values of M. The magnetic component design, carried out as a part of this work, indicates that I_{dc} and f_{sw} affects the sizing of the passive components. Higher I_{dc} drawn correlates to larger size of inductor as well as capacitor. Where-as the higher switching frequency translates in smaller size of the passive components.

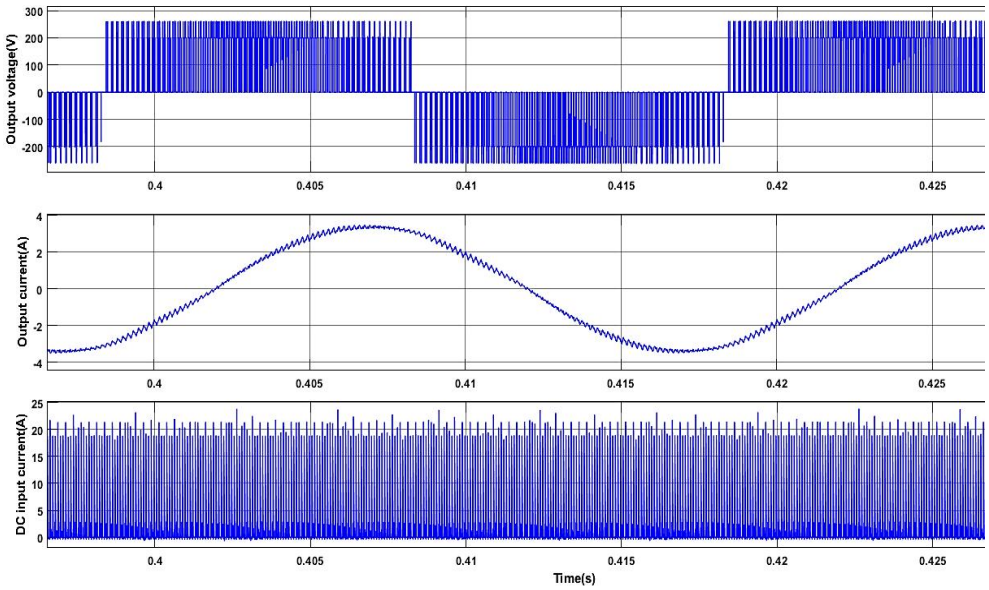

Fig. 3. Inverter output voltage and input current at 6 kHz switching frequency and 0.9 modulation index

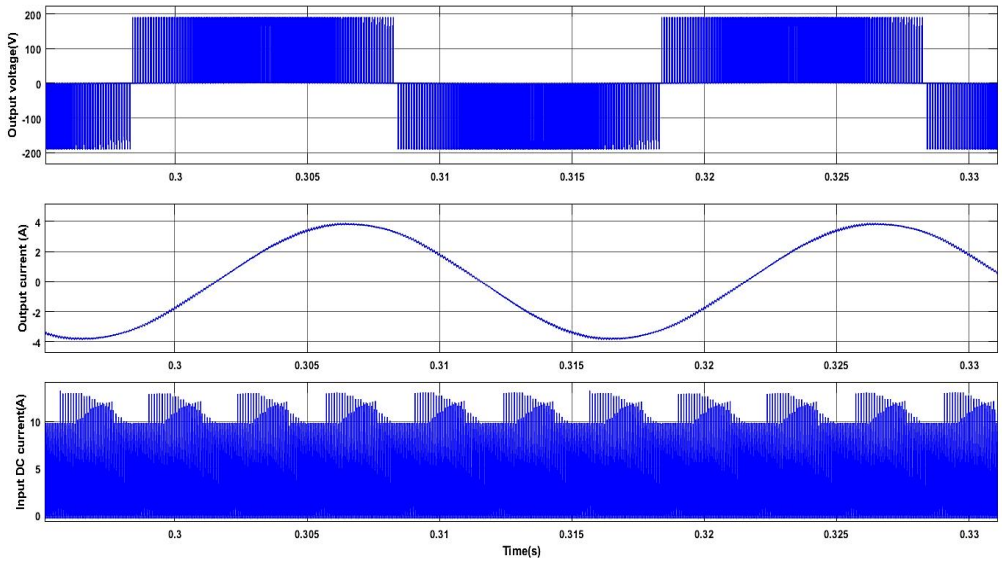

Fig. 4. Inverter output voltage and input current at 10 kHz switching frequency and 0.9 modulation index

Smaller the size of the passive components forming the impedance network of the ZSI, better the levels of efficiency as well as order of energy delivered at the output of the inverter which will suffice the need of the application. The constraint on size of the impedance network components leads to better chances of accommodating the said components in the hardware setup of the system where space constraint plays a vital role. The reduction in size of impedance network components on account of selection of higher switching frequency as well as modulation index

leads to significant reduction in the order of current drawn by the said network. This reduction in the value of current drawn contributes in reducing the order of losses incurred in the system as well as amount of heat generated by the system which indirectly affects the output range of the inverter in-general.

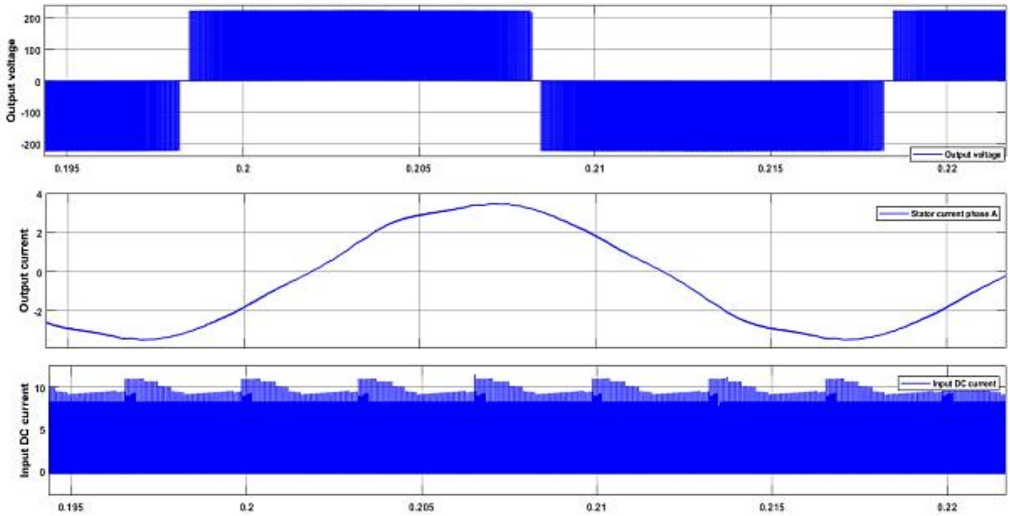

Fig. 5. Inverter output voltage and input current at 20 kHz switching frequency and 0.85 modulation index

Table 1
Result for shoot-through index of 0.9 at various switching frequencies

V_{dc} (V)	f_{sw} (kHz)	I_{dc} (A)	V_{in} (V)
140	6	24	233
140	8	15.8	190
140	10	13.8	185.5
140	12	11.5	178
140	14	11.9	178.1
140	16	9.7	172.5
140	18	10	170
140	20	9.1	166

Table 2
Output of inverter at different switching frequencies and shoot-through indices

V_{dc} (V)	M	f_{sw} (kHz)	I_{dc} (A)	V_{in} (V)
140	0.9	6	21	230
140	0.9	8	16.5	195
140	0.9	10	14	185
140	0.87	15	13	198
140	0.88	15	13	190
140	0.86	15	14	208
140	0.86	16	13.2	205
140	0.86	17	12.6	202
140	0.85	18	12.8	210
140	0.85	19	12.4	207
140	0.86	19	11.7	198
140	0.85	20	11.9	205

Further analysis for the same load at different switching frequencies and various shoot-through indices have also been carried out and the results are tabulated as follows. As clearly indicated in the mathematical relations, the variation in switching frequency leads to variation in output voltage of the inverter even if the modulation index is kept constant. Figure 6 shows trend for variation of output voltage with variation in switching frequency at 0.9 modulation index. Table 1 consolidates the above-mentioned variation. Similarly, the consolidated switching frequency variation and shoot-through index variation is tabulated in Table 2 below. The tabulated results and the exhibited waveforms provide an idea about the value of input current drawn from the source based on the value of modulation index as well as switching frequency selected. Based on this study, the rating and specification of the *dc* source which can act as a prospective source whose power can be extracted and integrated with the grid can be arrived upon. The said study also provides information about the suitability of the dc source like battery or photovoltaic module which can be integrated with the ZSI based on the order of current which is a function of the switching frequency and modulation index of the control strategy.

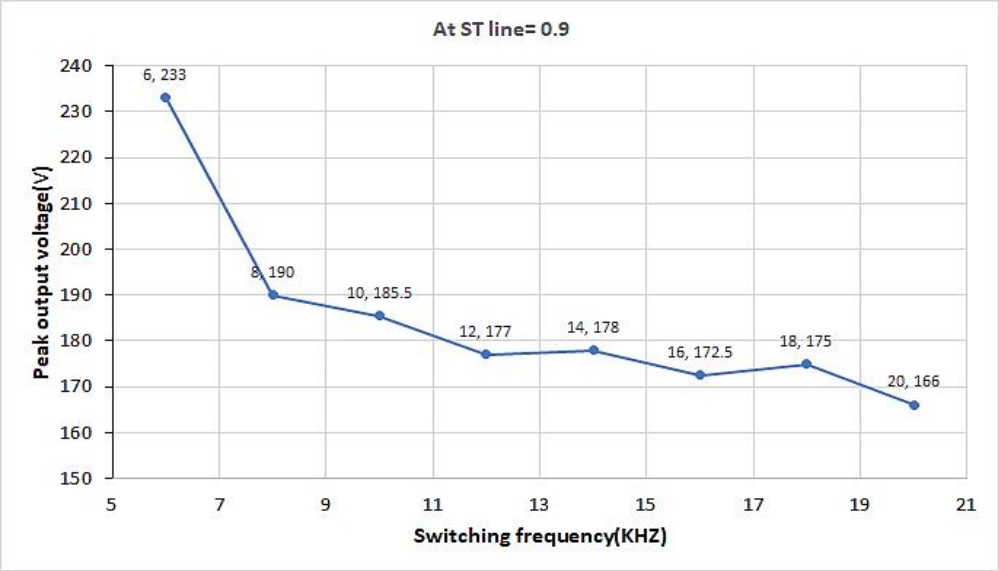

Fig. 6. Result analysis for 0.9 shoot-through index at different switching frequencies

4. Conclusions

The analysis and simulation results reveal that switching frequency and modulation index have significant impact on the value of current drawn by the VSI from the dc-link. The input dc current drawn by the converter as well as the switching frequency selected as part of control strategy affects the sizing of impedance network components. Higher dc current results in increased size of the inductor and capacitor as the stress on the component increased significantly. This is on account the fact that the input dc current drawn by the converter increases significantly with increase in the short circuit stage time duration. To be able to withstand the said short circuit current and be able to store the energy, a high amount of inductance is required. Similarly, this larger time duration of short circuit stage resulting in higher input dc current also increases the output ac voltage of the converter which is primarily due to higher dc voltage generated at the impedance network. This higher dc voltage has to be stored in energy form across the capacitor which eventually affects the sizing of capacitor too. As the current drawn, inductance value and

capacitance value is increased, the overall loss incurred during operation of the converter also increases leading to significant increment in the component sizing. Conversely, higher switching frequency results in reduced size of the passive components. A trade-off is expected to ensure that the output voltage of the ZSI is not compromised at the same time a higher input current is not drawn for a given range of switching frequency and modulation index. From the tabulated results, the best fit values are determined. In addition to this the results also helps in determining the rating and specifications of a potential dc source whose power can be drawn from and incorporated into the grid. The aforementioned study also provides details on the compatibility of the dc source, such as battery or photovoltaic module, which can be paired with the ZSI. The compatibility of the dc source, such as battery or photovoltaic module, depends on switching frequency and modulation index of the control strategy.

Acknowledgement
The study and findings presented in the article are the results of research that was conducted as part of a minor research project supported and funded by Nirma University in the fiscal year 2021–2022.

References

[1] Peng, Fang Zheng. "Z-source inverter." *IEEE Transactions on industry applications* 39, no. 2 (2003): 504-510. https://doi.org/10.1109/TIA.2003.808920
[2] Peng, Fang Zheng, Alan Joseph, Jin Wang, Miaosen Shen, Lihua Chen, Zhiguo Pan, Eduardo Ortiz-Rivera, and Yi Huang. "Z-source inverter for motor drives." *IEEE transactions on power electronics* 20, no. 4 (2005): 857-863. https://doi.org/10.1109/TPEL.2005.850938
[3] Peng, Fang Zheng, Miaosen Shen, and Zhaoming Qian. "Maximum boost control of the Z-source inverter." *IEEE Transactions on power electronics* 20, no. 4 (2005): 833-838. https://doi.org/10.1109/TPEL.2005.850927
[4] Yu, Kun, Fang Lin Luo, Miao Zhu, and Xu Cai. "Space vector pulse-width modulation theory and solution for Z-source inverters with maximum constant boost control." *International Journal of Circuit Theory and Applications* 42, no. 2 (2014): 127-145. https://doi.org/10.1002/cta.1842
[5] Kim, Seong Hwan, and Jang Hyun Park. "Maximum boost space vector pulse-width modulation strategy of Z-Source Inverters." *Journal of IKEEE* 19, no. 1 (2015): 73-79. https://doi.org/10.7471/ikeee.2015.19.1.073
[6] Ali, Hassan. "Z-source inverter fed induction motors." *International Journal of Industrial Electronics and Drives* 3, no. 2 (2016): 67-77. https://doi.org/10.1504/IJIED.2016.081578
[7] Rajakaruna, Sumedha, and Laksumana Jayawickrama. "Steady-state analysis and designing impedance network of Z-source inverters." *IEEE Transactions on Industrial Electronics* 57, no. 7 (2010): 2483-2491. https://doi.org/10.1109/TIE.2010.2047990
[8] Shunmugakani, P., and D. Kirubakaran. "Simulation and implementation of quasi-z-source based single-stage buck/boost inverter fed induction motor." *International Journal of Power Electronics and Drive Systems* 7, no. 2 (2016): 369. https://doi.org/10.11591/ijpeds.v7.i2.pp369-378
[9] Babaei, Ebrahim, Hitham Abu-Rub, and Hiralal M. Suryawanshi. "Z-source converters: Topologies, modulation techniques, and application–part I." *IEEE Transactions on Industrial Electronics* 65, no. 6 (2018): 5092-5095. https://doi.org/10.1109/TIE.2018.2793738
[10] Babae, E., H. M. Suryawanshi, and H. Abu-Rub. "Z-source converters: Topologies, modulation techniques, and applications—Part II." *IEEE Transactions on Industrial Electronics* 65, no. 10 (2018): 8274-8276. https://doi.org/10.1109/TIE.2018.2830218
[11] Tayab, U. B., M. A. Roslan, and F. N. Bhatti. "Comparative analysis of different switching techniques for cascaded h-bridge multilevel inverter." *Journal of Advanced Research in Computing and Applications* 3, no. 1 (2016): 1-6.
[12] El-Hamrawy, A. H., and A. I. Megahed. "Adaptive protection scheme for medium voltage systems with distributed generation and islanding detection." In *2017 Nineteenth International Middle East Power Systems Conference (MEPCON)*, p. 958-964. IEEE, 2017. https://doi.org/10.1109/MEPCON.2017.8301296
[13] Al Smin, Ahmed Moh A., Alkbir Munir Faraj Almabrouk, Sairul Izwan Safie, Mohd Al Fatihhi Mohd Szali Januddi, Mohd Fahmi Hussin, and Abdulgader Alsharif. "Enhancing solar hybrid system efficiency in Libya through PSO & flower pollination optimization." *Progress in Energy and Environment* (2024): 23-31. https://doi.org/10.37934/progee.27.1.2331

[14] Kong, Liang, and Heng Nian. "Transient modeling method for faulty DC microgrid considering control effect of DC/AC and DC/DC converters." *IEEE Access* 8 (2020): 150759-150772. https://doi.org/10.1109/ACCESS.2020.3017015

[15] Naas, Charak, Kouzou Abdallah, Khaidi Belgacem Said, and Nezli Lazhri. "Analysis of multi-phase qZ-Source Inverter with maximum constant boost control technique." *Electrotehnica, Electronica, Automatica* 69, no. 1 (2021). https://doi.org/10.46904/eea.21.69.1.1108005

[16] Kheyrati, Mohammad Reza, Amirhossein Rajaei, Vahid Moradzadeh Tehrani, Ghazal Mirzavand, and Mahdi Shahparasti. "A three-level single stage a-source inverter with the ability to generate active voltage vector during shoot-through state." *IEEE Access* 10 (2022): 31788-31799. https://doi.org/10.1109/ACCESS.2022.3160794

[17] Mande, Daouda, João Pedro Trovão, and Minh Cao Ta. "Comprehensive review on main topologies of impedance source inverter used in electric vehicle applications." *World Electric Vehicle Journal* 11, no. 2 (2020): 37. https://doi.org/10.3390/wevj11020037

[18] Ellabban, Omar, Joeri Van Mierlo, and Philippe Lataire. "Control of a bidirectional Z-source inverter for electric vehicle applications in different operation modes." *Journal of Power Electronics* 11, no. 2 (2011): 120-131. https://doi.org/10.6113/JPE.2011.11.2.120

[19] Ellabban, Omar, Joeri Van Mierlo, and Philippe Lataire. "Experimental study of the shoot-through boost control methods for the Z-source inverter." *EPE journal* 21, no. 2 (2011): 18-29. https://doi.org/10.1080/09398368.2011.11463792

[20] Sivapriyan, R., and S. Umashankar. "Comparative analysis of PWM controlling techniques of single phase Z-source inverter." *Indian Journal of Science and Technology* 9, no. 26 (2016). https://doi.org/10.17485/ijst/2016/v9i26/92210

[21] Iijima, Ryuji, Naoki Kamoshida, Rene Alexander Barrera Cardenas, Takanori Isobe, and Hiroshi Tadano. "Evaluation of inductor losses on z-source inverter considering AC and DC components." In *2018 International Power Electronics Conference (IPEC-Niigata 2018-ECCE Asia)*, pp. 1111-1117. IEEE, 2018. https://doi.org/10.23919/IPEC.2018.8507925

[22] Dong, Shuai, Qianfan Zhang, and Shukang Cheng. "Inductor current ripple comparison between ZSVM4 and ZSVM2 for Z-source inverters." *IEEE Transactions on power electronics* 31, no. 11 (2015): 7592-7597. https://doi.org/10.1109/TPEL.2015.2475614

[23] Sreeprathab, N. R., and X. Felix Joseph. "A survey on Z-source inverter." In *2014 International Conference on Control, Instrumentation, Communication and Computational Technologies (ICCICCT)*, p. 1406-1410. IEEE, 2014. https://doi.org/10.1109/ICCICCT.2014.6993182

[24] Shen, Miaosen, Jin Wang, Alan Joseph, Fang Zheng Peng, Leon M. Tolbert, and Donald J. Adams. "Constant boost control of the Z-source inverter to minimize current ripple and voltage stress." *IEEE transactions on industry applications* 42, no. 3 (2006): 770-778. https://doi.org/10.1109/TIA.2006.872927

[25] Tang, Yu, Shaojun Xie, Chaohua Zhang, and Zegang Xu. "Improved Z-source inverter with reduced Z-source capacitor voltage stress and soft-start capability." *IEEE transactions on power electronics* 24, no. 2 (2009): 409-415. https://doi.org/10.1109/TPEL.2008.2006173